

Check for updates





Mulching During Boreal Resource Development Alters Near-Surface Hydrophysical Properties and Triggers **Episodic Methane Emissions in Peatland Soils**

Nicole E. Balliston 🕒 | Marissa A. Davies | Kayla J. Martin | Maria Strack 🗓

Department of Geography and Environmental Management, University of Waterloo, Waterloo, Ontario, Canada

Correspondence: Nicole E. Balliston (nballiston@uwaterloo.ca)

Received: 15 October 2024 | Revised: 11 February 2025 | Accepted: 17 March 2025

Funding: This work was supported by Environment and Climate Change Canada.

Keywords: carbon cycling | greenhouse gas fluxes | hydrophysical structure | linear disturbance | methane emissions | mulching impacts | peatlands

ABSTRACT

Linear disturbances within boreal Canada (e.g. seismic lines) can significantly disrupt carbon cycling in northern peatlands, potentially transforming these significant carbon stocks from long-term carbon sinks into net carbon sources. Recent efforts have been made to quantify the impacts of linear disturbance on vegetation, soil composition and greenhouse gas (GHG) emissions. However, little is known about the specific interactions between disturbances to peat hydrophysical structure and composition and the resulting alterations to CO₂ and CH₄ dynamics. To this end, eight poor fen peat cores were collected on, and eight cores collected adjacent to a seismic line representing the top 10 cm of the peat profile. These cores reflected four degrees of disturbance, with four cores per treatment: complete mulch covering, partial mulch covering, mechanical roughing only and undisturbed. In controlled laboratory conditions, cores were subjected to two subsequent static water table conditions (3 and 8 cm below the core surface) for ~30 days each with GHG flux measurements occurring every 2-3 days. Cores were then subdivided into 5 cm segments and underwent hydrophysical (i.e., bulk density, porosity and water retention) and compositional (i.e., C:N and vegetational assemblage) analysis. Results show that peat composition and hydrophysical structure were both strong predictors of GHG emissions. Higher CO2 emissions were related to peat with high bulk density, low total and effective porosity and low C:N ratios, which occurred at depth in the undisturbed cores and at the surface where mechanical mulching and mixing occurred. Increased CH4 emissions occurred in a subset of disturbed cores characterized by a reduction in macropores and effective porosity near the surface; these emissions were episodic and occurred where trapped gas was released. Further fieldscale research is needed to evaluate the interrelationships between the direct impacts of seismic line creation on hydrophysical structure and composition and the long-term changes in carbon cycling within disturbed systems.

1 | Introduction

Canada's peatlands store a significant portion of the global northern peatland carbon pool and act as a net carbon sink due to the slow millennial-scale accumulation of organic-rich soils under waterlogged conditions (Frolking and Roulet 2007; Hugelius et al. 2020). However, these ecosystems are increasingly vulnerable to anthropogenic pressures such as industrial activities, agriculture and urban expansion, which alter their ecohydrological conditions and may shift them from carbon sinks to net sources (Loisel and Gallego-Sala 2022). Understanding how disturbances impact peatland carbon cycling is essential to accurately quantify greenhouse gas (GHG) fluxes and improve land-use emission estimates (IPCC 2014).

This is an open access article under the terms of the Creative Commons Attribution-NonCommercial License, which permits use, distribution and reproduction in any medium, provided the original work is properly cited and is not used for commercial purposes

© 2025 The Author(s). Ecohydrology published by John Wiley & Sons Ltd.

Peatlands exhibit complex CO_2 and CH_4 dynamics influenced by interactions between peat hydrophysical structure, physiochemical composition and environmental conditions. During periods of reduced water availability, lowered water tables increase air-filled pores and facilitate aerobic respiration and CH_4 oxidation (Clymo 1983; Howard and Howard 1993; Waddington et al. 1996; Blodau et al. 2004). Conversely, during periods of high water availability, raised water tables saturate pore spaces, limiting oxygen availability and promoting CH_4 -generating anaerobic decomposition (Bridgham et al. 2013; Bubier et al. 1993).

Moisture dynamics are further complicated in near-surface peat (i.e., the acrotelm; Ingram 1978), where the structure changes rapidly with depth. Near the surface, pores are large, open and well connected, draining readily above the water table (Price et al. 2008; Goetz and Price 2015; Rezanezhad et al. 2010, 2016). Consequently, rates of CO₂ production and CH₄ oxidation are generally higher, whereas CH₄ production is lower (Clymo and Pearce 1995; Clymo 1996). As the degree of decomposition increases with depth (Hayward and Clymo 1982), peat becomes more compact, with smaller pores, higher bulk density and increased water retention upon drainage (Boelter 1969; Quinton et al. 2009). These conditions limit oxygen availability and enhance CH₄ production, with maximum rates typically occurring 10-20cm below the water table (Sundh et al. 1994; Kettunen et al. 1999). At greater depths, peat becomes more humified and recalcitrant, reducing labile carbon availability and slowing mineralization (Hogg et al. 1992; Updegraff et al. 1995) and decomposition (Hogg 1993) rates. In undisturbed peatlands, vertical connectivity is maintained with a gradual transition in soil hydraulic properties with depth (Nungesser 2003). However, disturbance can disrupt this structure, altering carbon cycling dynamics (e.g. Bieniada and Strack 2021).

Reporting on GHG emissions from peatland disturbances in Canada has improved in recent years, but significant gaps remain. Resource extraction, a significant driver of land conversion in the boreal region (Wilkinson et al. 2023), is currently underrepresented in emissions reporting. Among resource extraction-related disturbances, seismic lines (grid-patterned linear clearings for geophysical surveys) are particularly impactful, spanning 1.5–1.8 million km in boreal Canada (Dabros et al. 2018) and affecting >1900 km² of peatlands in Alberta alone (Dabros et al. 2018; Strack et al. 2019). Seismic lines disrupt vegetation and soil structure, raise water tables and alter carbon cycling.

Modern 'low-impact' seismic lines (LIS), typically created during the winter using low ground-pressure mulchers or lightweight machinery, are narrower (2–4 m) and less disruptive than historical methods, which involved heavier equipment and wider clearings (Dabros et al. 2018). However, LIS still remove vegetation communities (Severson-Baker 2003; van Rensen et al. 2015), can potentially compress and/or mix soils (Severson-Baker 2003; Davidson et al. 2020) and reduce microtopography (Lovitt et al. 2018). These changes can raise water tables (van Rensen et al. 2015) and increase soil moisture (Williams et al. 2013; Davidson et al. 2020), potentially enhancing $\mathrm{CH_4}$ fluxes compared to adjacent peatlands (Strack et al. 2018). Seismic line peat samples also show lower carbon-to-nitrogen ratios, indicative of enhanced decomposition, shifts

in vegetation composition and/or the addition of woody debris (Davidson et al. 2020). Without intervention, these effects can persist for decades. Limited spontaneous recovery is observed in seismic lines, with woody vegetation regrowth often lagging by over a decade or remaining in early successional stages (Lee and Boutin 2006). Although most research has focused on seismic lines, similar impacts have also been reported on forestry cutlines and trails (Lepilin et al. 2019) and oil sands' exploration well sites (Caners and Lieffers 2014; Murray et al. 2021).

Despite evidence linking seismic line disturbances to altered peatland carbon cycling, little research has directly explored how changes in peat composition and hydrophysical structure affect ${\rm CO_2}$ and ${\rm CH_4}$ fluxes. Although previous studies have demonstrated that disturbances can increase soil respiration by introducing labile carbon and nutrients (Larmola et al. 2013; Weedon et al. 2013), the impacts of mechanical disturbance and woody material incorporation from mulching on peat hydrophysical properties and carbon fluxes remain poorly understood. Findings from this study can also inform the management of other boreal peatland disturbances, such as road creation, and electricity transmission and pipeline corridors, which share similar effects on vegetation and hydrophysical conditions.

Therefore, the goal of this work is to better understand how natural and disturbance-induced differences in peat composition and hydrophysical structure relate to observed GHG cycling while controlling for environmental variation in a laboratory setting. The specific objectives are to (1) assess the difference in ${\rm CO}_2$ and ${\rm CH}_4$ fluxes between undisturbed and seismic line impacted peat, (2) characterize and assess the variability of near-surface peat composition and hydrophysical structure as a function of natural heterogeneity and disturbance and (3) relate observed differences in carbon fluxes to natural and disturbance-induced variability in peat composition and hydrophysical structure.

2 | Materials and Methods

2.1 | Sample Location, Collection and Preparation

The study site is a poor fen within a larger peatland complex located on an active lease 150 km south of Fort McMurray, Alberta, Canada (Kirby South; 55.37°N, 111.15°W; Figure 1). The seismic line where the samples were collected was created over the winter of 2021–2022 and field sampling was performed on 13 July 2022. The line was on average 4 m wide and was created using a mulcher.

A total of 16 cylindrical peat cores (10 cm diameter) representing the top 10 cm of the peat profile were collected in PVC tubing from two seismic lines and their adjacent reference locations. The four reference (CON) cores were collected 10–15 m from the seismic line (2 at each reference location) and were divided into two treatments: two *Sphagnum* moss-dominated control replicates (CON-SPH) and two feathermoss-dominated control replicates (CON-FEA). Samples were taken at a maximum distance of 10–15 m from a disturbance, as this was the furthest distance achievable under the site conditions given the high density of seismic lines in the area. Twelve cores were collected to represent disturbed conditions. Of these,

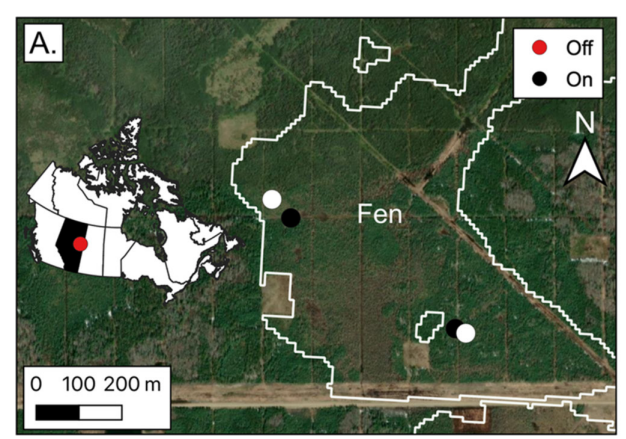




FIGURE 1 | Sample collection location for this study. (A) Locations of samples collected from the mulched seismic lines (on) and reference areas (off). The red dot indicates the general location in northern Alberta, Canada. The delineation of the fen area is from the ABMI Wetland Inventory (ABMI 2021). Base map from ESRI World Imagery (Maxar (Vivid) Imagery, 1 pixel = 0.5 m, 1 August 2018). (B) Image from northernmost seismic line site in A. Photo credit: M. Strack.

two *Sphagnum* moss-dominated cores were taken from each reference location and mechanically roughed (RGH-SPH) in the lab to mimic the effects of surface disturbance in the absence of mulch incorporation (4 cores total). A total of eight cores were collected across the two seismic lines to represent a combination of mulching and surface disturbance. Four of these cores represented peat which was partially covered by mulched black spruce trees (MUL-LOW) and four that were entirely covered in mulched trees (MUL-HI) and represented the edge and centre of the seismic line, respectively.

2.2 | Experimental Conditions and Carbon Dioxide and Methane Flux Measurements

Prior to the experiment commencement, the 16 cores were divided into two insulated coolers where they were secured upright with random placement (Figure S1). Deionized water was initially added to each cooler to achieve a water table depth of 8 cm above cooler bottom (~3 cm below core surface), herein referred to as the wet condition. Cores were allowed to stabilize for 1 week prior to the start of flux measurements. Apart from flux measurement days, cooler lids were left 90% closed to reduce evaporation and temperature fluctuations while promoting air circulation and thus minimizing ${\rm CO_2}$ and ${\rm CH_4}$ accumulation. Throughout the duration of the experiment, water levels were measured daily and topped up with deionized water to maintain water level stability.

The wet condition of the core experiment officially commenced on 25 January 2023, which coincides with the first round of flux measurements. In total, $\rm CO_2$ and $\rm CH_4$ fluxes were measured on Days 1, 2, 6, 9, 13, 16, 20 and 23 using the closed chamber method with a 1.81 L chamber affixed to the top of the core by a custom tubing attachment and sealed for 3 min. Concentrations in the headspace were measured with a $\rm CO_2/CH_4$ infrared trace gas analyser (LI-COR; LI-7810; Lincoln, NE, USA). Water was then removed from the coolers until a new water table height of 3 cm above cooler bottom (~8 cm below core surface) was achieved (herein referred to as dry condition) and allowed to equilibrate for 1 week. After

equilibration, fluxes were then measured on Days 1, 4, 7, 9, 14, 17 and 21 of the dry experimental conditions. For both wet and dry conditions, cooler lids were first opened prior to flux measurement to allow for the dissipation of any trapped gases. Room temperature, relative humidity and water levels at the time of flux measurements were recorded at the time of each flux to account for slight variability.

 ${\rm CO}_2$ and ${\rm CH}_4$ fluxes were calculated using a linear fit through the measured gas concentration change through time (ppm s⁻¹) and then converted to a change in mass using the ideal gas law (PV = nRT). Standard atmospheric pressure and the temperature at the time of measurement were used in the conversion.

2.3 | Characterization of Hydrophysical and Soil Properties

After experiment completion, each box was drained, and all cores were immediately wrapped in cling wrap and frozen to prevent further decomposition prior to analysis. Each core was then subdivided into two sub-cores (top and bottom) while frozen representing the 0–5 cm and 5–10 cm depth intervals, respectively. All soil property analysis was completed separately on each sub-core to better understand depth related processes and impacts of disturbance.

2.3.1 | Hydrophysical Properties

Prior to the determination of hydrophysical properties, subcores were first thawed and saturated in deionized water for a minimum of 48 h. The saturated volume and weight of each subcore were then measured. Water retention was characterized at $-7.5 \, \mathrm{cm}$ (5 cm below the bottom of each core) using a soil water retention table and at $-100 \, \mathrm{cm}$ using the pressure plate method outlined by McCarter and Price (2017). Using the capillary rise equation (Bear 1972) and assuming a contact angle of 51° (Gharedaghloo and Price 2019), the equivalent saturated pore size for each pressure step was determined to be 265 and $20 \, \mu \mathrm{m}$

at -7.5 and -100 cm, respectively. Pores greater than $265\,\mu m$ can be considered representative of macropores (commonly measured as $>100\,\mu M$; Holden 2009), whereas a $20\,\mu m$ pore size is generally used as the boundary between pores that are closed and open to flow (McCarter and Price 2017). The fraction of water-filled pores at each pressure step (i.e., the fraction of pores at a given size range dictated by the previous and current pressure steps) was determined as

$$\emptyset_{vw} - = \frac{\theta(\psi)}{n_t}$$

where \emptyset_{vw} is the proportion of saturated pores (–), θ is the water content (–) at pressure ψ and n_t is the total porosity, assumed to be the water content at 100% saturation (ψ = 0).

Volumetric water content at all pressure conditions including saturation was determined as

$$\theta(\psi) = \frac{\left(M_{\psi} - M_{dry}\right)}{V_{t(\psi)}\rho_w}$$

where M_{Ψ} is the sub-core mass at a given pressure (g), M_{dry} is the dry sub-core mass (g), $V_{t(\Psi)}$ is the total sub-core volume at a given pressure (cm³), and ρ_{W} is the density of water. Dry mass was determined by weighing each sub-core after oven drying at 60°C for 48 h. Saturated and dry bulk densities were calculated by dividing the mass at each pressure by the sub-core volume.

The change in core volume between each pressure was determined as

$$\Delta \mathit{V} \big(\psi_x \big) = V_{t(x-1)} - \mathit{V}_{t(x)}$$

where $V_{t(x-1)}$ is the volume of the sub-core at the previous pressure and $V_{t(x)}$ is the volume at the current pressure.

Total porosity was determined as

$$n_t = 1 - \frac{\rho_d}{\rho_p}$$

where n_t is the total porosity (–), ρ_d is the dry bulk density (g/cm³) and ρ_p is the particle density (g/cm³). The particle density was measured using the soil volume displacement method with kerosene as a substitute for water due to the hydrophobic nature of dry peat (Whittington et al. 2021). Effective porosity (n_e) was assumed to be equal to the volume of pores filled at –100 cm in accordance with McCarter and Price (2017).

2.3.2 | Peat Geochemistry and Plant Composition

To determine peat total carbon and nitrogen mass in each of the cores, approximately 1–2 g of dried material from each core subsection was ground to a fine powder with a Retsch ball mill (N=32). From the ground material, 1–2 mg of the homogenized sample was analysed for C and N (%) using a Costech 4010 elemental analyser coupled to a Thermo Finnigan Delta Plus XL continuous flow

isotope ratio mass spectrometer at the Environmental Isotope Lab at the University of Waterloo, Canada. Replicates were within 5% for C and 2% for N, respectively (N=11). Carbon content was multiplied by the total dry mass (g) for each subsection and was combined to determine the total mass of each core. The total carbon content in the core was used to normalize the carbon fluxes to g C-CO₂/g C-peat/day and mg C-CH₄/g C-peat/day.

Peat plant composition was determined on the > 300 µm fraction of a 5 cm³ subsample from each core subsection (N=32) using a modified quadrat method described by Mauquoy et al. (2010). A total of five 2×2cm squares within a gridded petri dish were counted at 20× magnification on a stereomicroscope for each sample. The major vegetation groups counted were ericaceous leaves, woody roots, large wood fragments, herbaceous plant fragments, Sphagnum stems and leaves, feathermoss stems and leaves, brown moss stems and leaves, conifer needles and unidentified organic material (UOM). Counts were converted to percentages based on the total plant fragments counted for each sample. Major vegetation groups were identified by referencing Lévesque et al. (1988). Each sample was then assigned to a peat type, based on the major vegetation groups. If a vegetation group was greater than 10% of the peat plant composition, then it was assigned that peat type. The four peat types in this study were Sphagnum (SPH), Sphagnum and woody roots (SPH-ROOT), feathermoss and woody roots (FEA-ROOT) and woody roots (ROOT).

2.3.3 | Statistical Testing

To test significant differences in both gas fluxes and hydrophysical properties across different treatments and/or moisture conditions, datasets were analysed statistically using R software (R Core Team 2021) and the *dplyr* analysis package. All datasets were first tested for normality using the Shapiro–Wilk normality test; where datasets were normal, a one-way analysis of variance (ANOVA) was then used to test for significant differences between distributions, whereas non-normal datasets were analysed using the Kruskal–Wallis test. Post hoc analysis was used to assess differences between individual treatments and/or moisture conditions using the Tukey analysis and Dunn analysis for normal and non-normal datasets, respectively.

Non-metric multidimensional scaling (NMDS) was performed to investigate linkages between soil hydrophysical properties and peat plant composition. Peat plant composition was standardized to proportions and square root transformed prior to analysis (Hellinger transformation; Legendre and Legendre 2012). The NMDS was performed using the 'metaMDS' function in the vegan package in R and was based on Bray-Curtis dissimilarity (k = 2; autotransform = FALSE; Oksanen et al. 2018). Surfaces for the hydrophysical properties (bulk density, C:N ratio and total and effective porosity) were fit to the NMDS post hoc and were tested for significance using the 'envfit' function in the vegan package in R (N=999permutations; Oksanen et al. 2018). Surfaces for CO₂ and CH₄ fluxes across the entire experiment were also fitted using the same method, where the average value of the wet and dry treatment for each core was assigned to both the top and bottom segments. All raw data collected and used in statistical analysis are available as Supporting Information.

3 | Results

3.1 | GHG Fluxes

All core replicates and treatments acted as CO_2 sources (i.e., exhibited net positive fluxes) throughout the experiment (Figure 2a). Within treatments, median CO_2 fluxes were generally higher under the dry condition compared to the wet condition; however, this difference was statistically significant (p < 0.01) only in the MUL-HI treatment (Tables S1–S3). Between treatments, CO_2 fluxes were significantly lower in the Sphagnum-dominated reference cores (CON-SPH) compared to feathermoss-dominated reference cores (CON-FEA), across both water table conditions. For the impacted cores, the roughed Sphagnum treatment (RGH-SPH) exhibited CO_2 fluxes similar to CON-SPH, whereas the mulched treatments (MUL-HI and MUL-LOW) showed flux distributions and medians similar to CON-FEA (Figure 2a; Tables S2 and S3).

Variation in $\mathrm{CH_4}$ fluxes within and across treatments differed markedly between the two water table conditions (Figure 2b). Under the wet condition, no significant differences were observed among treatments (Tables S1 and S2), and all treatments acted as $\mathrm{CH_4}$ sources on average throughout the experiment (Table S3). In contrast, during the dry condition, the average and standard deviation of $\mathrm{CH_4}$ fluxes were one to two orders of magnitude higher than in the wet condition (Table S3), with more pronounced differences between treatments (Figure 2b). Fluxes in the RGH-SPH treatment were significantly lower than in all other treatments (Table S2), and it was the only treatment to function as a net $\mathrm{CH_4}$ sink on average (Figure 2b and Table S3).

No significant differences in median CH4 fluxes were observed between the mulched treatments and the control cores (Figure 2b and Table S2). However, average CH, fluxes in MUL-LOW and MUL-HI were an order of magnitude higher than in CON-SPH and CON-FEA (Table S3). These averages were strongly influenced by individual cores (Table S4) and specific flux events (outliers in Figure 2b). For example, in the MUL-HI treatment, a single core (MUL-HI-2; Table S4) contributed 99% of the total flux for this treatment, with three disproportionately large flux events accounting for 81% of this value. A similar but less extreme bias occurred in the MUL-LOW treatment, where two of the four cores (MUL-LOW-2 and MUL-LOW-4; Table S4) accounted for 49% and 43% of the total treatment flux, respectively. Each of these cores experienced two disproportionately large flux events, each contributing 10%-15% of the total flux for this treatment.

3.2 | Peat Plant Composition and Geochemistry

The major vegetation groups found within each core matched the field categorization, with the largest amount of variability present in the seismic line samples where mulch cover obscured moss identification. Consistent with field observations, top and bottom *Sphagnum* treatments (CON-SPH and RGH-SPH) contained the largest % of *Sphagnum* stems and leaves of all treatments (Figures 3 and S2), with a slight decline in the proportion *Sphagnum* and a corresponding increase in woody root material between the top and bottom sub-cores. Contrastingly, whereas the feathermoss-dominated cores (CON-FEA) were mostly feathermoss in the top sub-core, the bottom sub-core of this treatment did not remain consistent and was dominated by either *Sphagnum* or

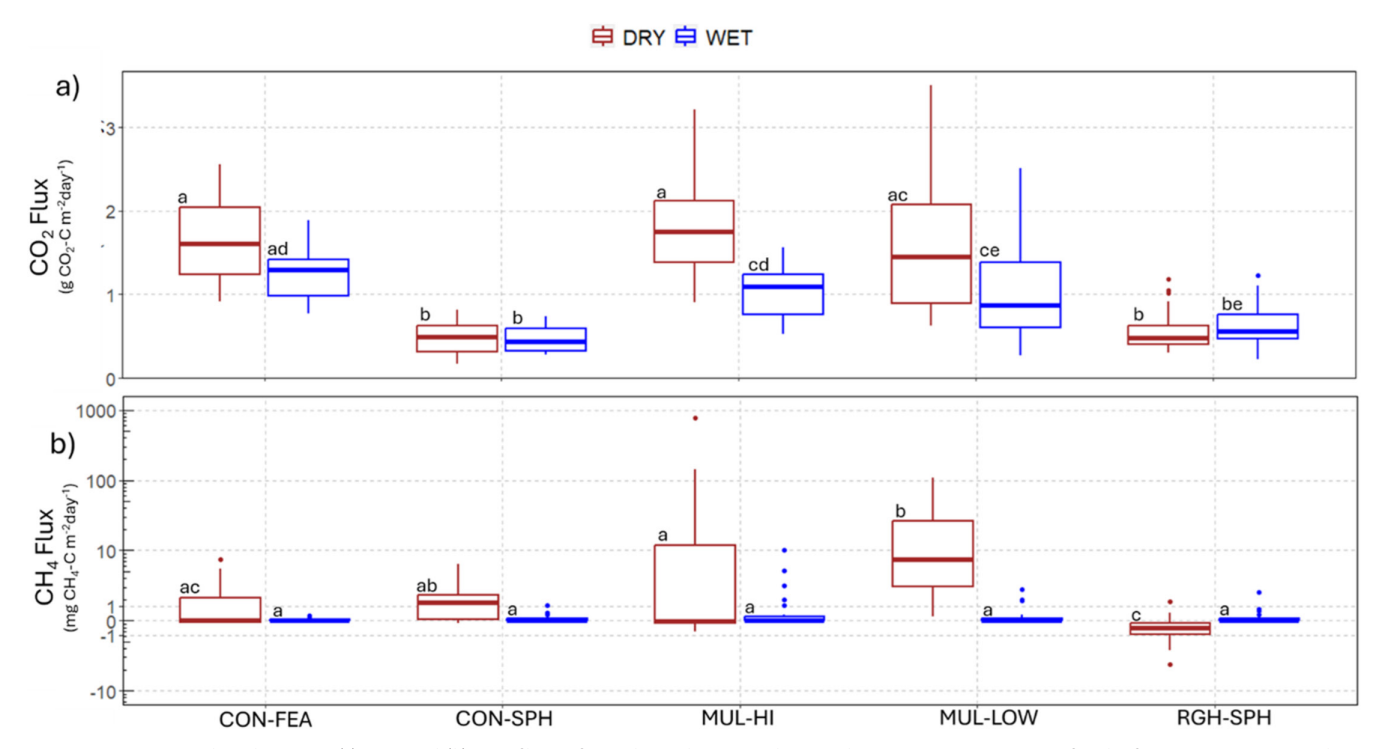


FIGURE 2 | Boxplots depicting (a) CO₂ and (b) CH₄ fluxes from the eight wet and seven dry measurement events for the five treatments. Matching letters indicate distributions that are not significantly different at the 95% confidence interval.

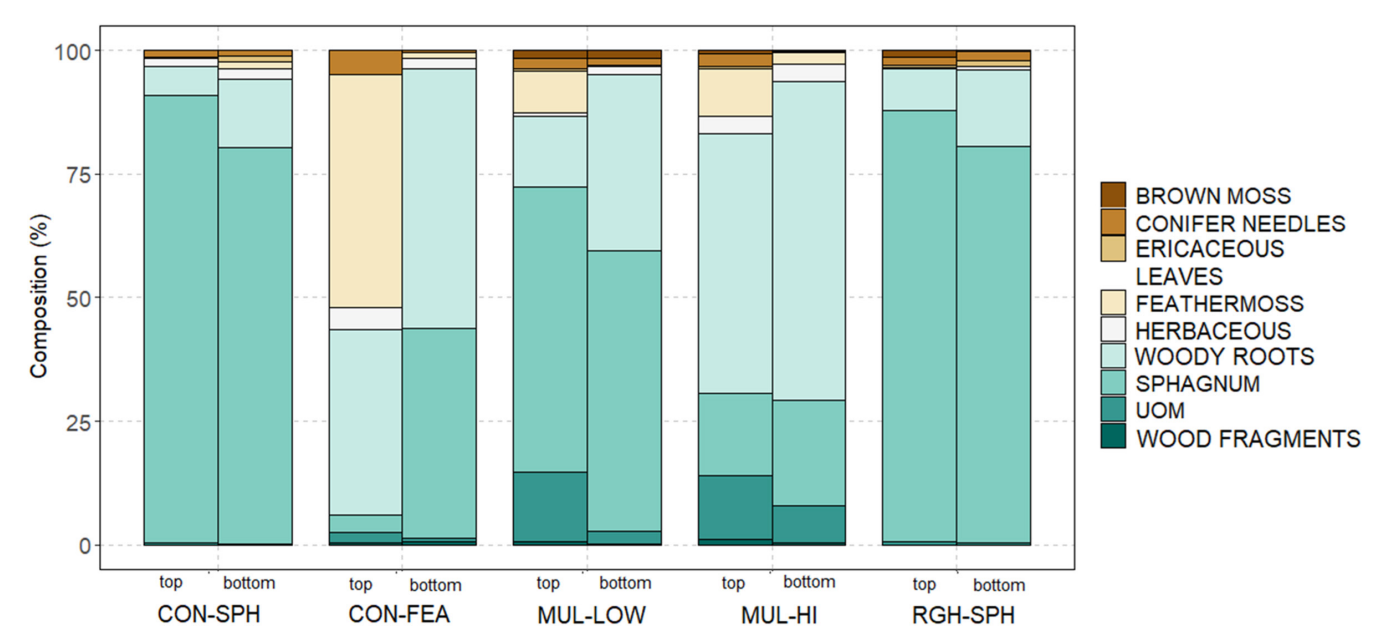


FIGURE 3 | Plant composition assemblages for top and bottom cores of each of the five treatments averaged over each category's replicates.

TABLE 1 | Treatment top and bottom sub-core and full core % carbon, % nitrogen and C:N ratio averaged over all replicates.

	Top 5 cm			Bottom 5 cm			Core average
	C (%)	N (%)	C:N	C (%)	N (%)	C:N	C:N
CON-SPH	45	0.5	90:1	44	0.4	108:1	99:1
CON-FEA	49	0.7	69:1	48	0.7	70:1	70:1
RGH-SPH	46	0.6	88:1	45	0.4	120:1	104:1
MUL-LOW	46	0.7	89:1	46	0.7	69:1	79:1
MUL-HI	48	0.8	58:1	49	0.8	61:1	60:1

woody roots. Compared to the controls, MUL-LOW and MUL-HI cores had lower proportions of mosses and higher proportions of root material and unidentified organic material (UOM). Though on average MUL-HI had the least *Sphagnum* and most rooting material of all treatments, there was a large degree of variability between individual cores (Figure S2).

The C:N ratios were different across the various treatments and depended on the dominant moss type (Tables 1 and S5). In the controls and roughed *Sphagnum* treatments (i.e., non-mulched treatments), C:N ratios increased with depth and were ~1.5× higher in the *Sphagnum*-dominated treatments than those dominated by feathermoss. The average top and bottom C:N ratios in the semi-mulched treatment decreased with depth but were within the range of the control treatments, whereas both top and bottom C:N ratios in the entirely mulched treatment fell below all other treatments. Inter-sample variability was notably lower in the control treatments when compared to the disturbed (Table S5).

3.3 | Hydrophysical Properties

Across all treatments, total porosity (n_l) , effective porosity (n_e) and % macropores $(\%_m)$ generally decreased with

depth, with a corresponding increase in dry bulk density (ρ_d) (Figure 4a–d; associated retention curves in Figure S3). Within the control treatments, the degree to which properties changed with depth differed. Although top sub-cores were similar between feathermoss and *Sphagnum* controls, there was a substantial change in n_e , \mathcal{H}_m and ρ_d with depth in CON-FEA compared to relatively subtle changes within CON-SPH. Specifically, ρ_d increased by 30% in CON-SPH and 200% in CON-FEA, whereas \mathcal{H}_m decreased by 15% in CON-SPH and 50% CON-FEA, respectively.

Hydrophysical properties were highly variable within (point values in Figure 4) and between the impacted treatments. Of the disturbed treatments, properties were the least variable and most similar to the controls in RGH-SPH; values in this treatment were comparable to CON-SPH though variability was higher between individual samples. The influence of disturbance was more apparent in the mulched cores; both MUL-LOW and MUL-HI treatments had a denser peat structure with lower n_t , n_e and \mathcal{S}_m , particularly in the top sub-core. Bulk density was highest and measures of porosity lowest in MUL-HI; however, there was much overlap between the two mulched treatments.

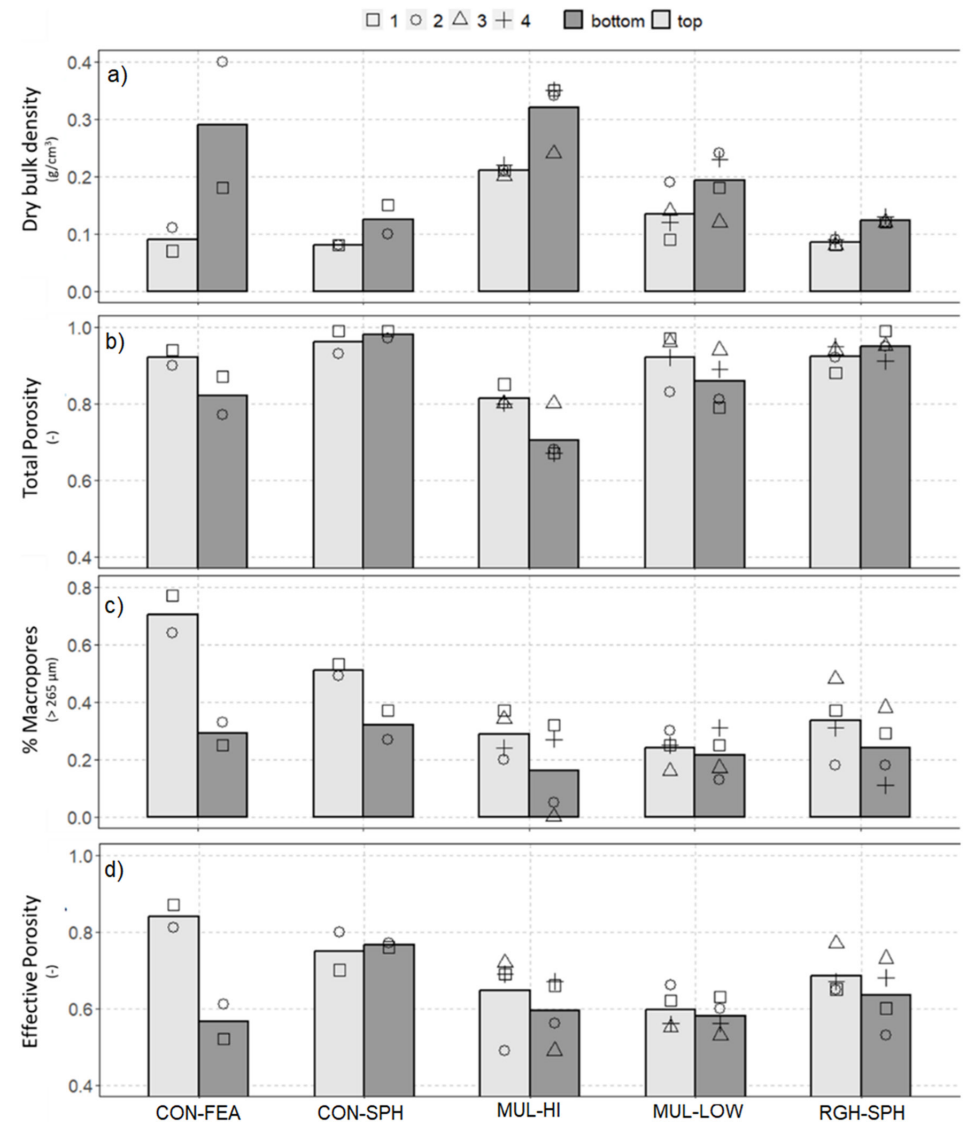


FIGURE 4 | Top (0–5 cm) and bottom (5–10 cm) sub-core: (a) dry bulk density (ρ_d), (b) total porosity (n_t), (c) % macropores ($\%_m$) and (d) effective porosity. Averages for each treatment are denoted by grey-filled boxes and individual values from replicates by points.

3.4 | Relating Core Peat Type, Hydrophysical Properties and GHG Fluxes

 CO_2 and CH_4 fluxes were strongly linked to core hydrophysical properties and peat type, as shown by the NMDS ordination (Table S6 and Figure 5). Under both wet and dry conditions, cores with greater proportions of *Sphagnum* had a higher C:N ratio and lower CO_2 fluxes (Table 1 and Figures 2 and 5). In contrast, cores with higher proportions of other components, especially UOM, herbaceous materials and woody roots, showed higher CO_2 fluxes.

An inverse relationship between flux and effective porosity in the top sub-core was the only significant hydrophysical determinant of CH_4 flux in both dry and wet. By composition, larger CH_4 fluxes were correlated with a higher woody root material (Figures 2 and 3); cores with this composition also exhibited a higher ρ_d and low n_t and \mathcal{S}_m (Figure 4 and Table S5).

4 | Discussion

4.1 | CO₂ Dynamics and the Influence of Hydrophysical Structure and Disturbance

Generally, both disturbed and undisturbed CO_2 fluxes (Figure 2 and Table S3) fall within the lower end of literature values derived from previous mesocosm flux experiments using bog and poor fen peat (Figure 6a; Moore and Dalva 1993; Blodau et al. 2004; Dinsmore et al. 2009; Deppe et al. 2010; Estop-Aragonés et al. 2016). The cores used for this experiment were notably shorter than in reference literature; when normalized by core height (g CO_2 C/m³/day) our fluxes were up to 2 orders of magnitude larger than literature values (Figure 6a). This is likely due to the decreasing contribution of peat to CO_2 flux with depth as labile carbon becomes depleted (Strack et al. 2017). This is supported by a significant negative relationship between experiment core height and normalized CO_2 flux across this and literature values (r^2 = 0.25, p < 0.01; see also Figure S4). The lack of a statistically significant increase in CO_2 flux with increasing

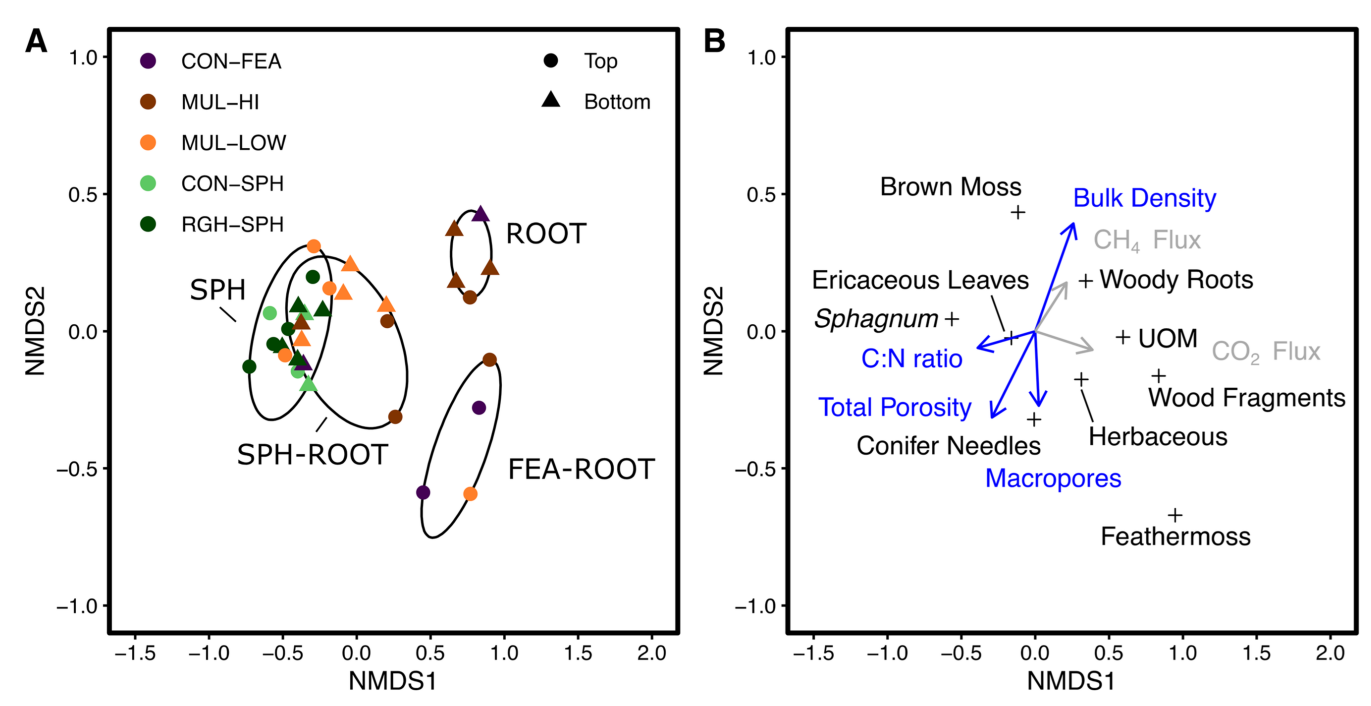


FIGURE 5 | NMDS biplots for peat plant composition of the cores taken on and off a seismic line in Kirby South, northern Alberta, Canada (N=36 samples; k=2, stress=0.082). (A) Site scores are sorted by treatment and position within the core. Circles surrounding sample points represent the area surrounding the centroid for a given peat composition type that includes all core samples of that given type. (B) Peat properties (blue) and carbon fluxes (grey) plotted as vectors that had a significant relationship between NMDS axes 1 and 2 (see Table S6 and species scores for each vegetation group identified in the peat cores).

water table depth in most treatments (Figure 2 and Table S2) was unexpected, as generally the widening of the oxic zone, is correlated with increased ${\rm CO_2}$ emissions (Blodau et al. 2004; Dinsmore et al. 2009). One potential explanation is the relatively shallow water table in the dry condition (8 cm bgs) could have limited the potential for air entry into the peat profile, thus muting this relationship. Previous studies have also shown that there can be an insensitivity of ${\rm CO_2}$ flux where there are overriding variations of peat composition (Moore and Dalva 1993) and hydrophysical structure, consistent with the strong correlations with these variables in this study (Figure 5 and Table S6).

CO, fluxes were strongly related to both natural and disturbance-induced variations in peat composition and hydrophysical structure. The specific drivers of CO₂ flux, however, differed between the disturbed and undisturbed treatments. In the undisturbed treatments, feathermoss-dominated cores quickly transitioned from top sub-cores with low ρ_d , high n_t and $n_{\scriptscriptstyle o}$ to bottom sub-cores, which were of high $\rho_{\scriptscriptstyle d}$ and low porosity (Figure 4), which resulted in elevated fluxes when compared to the Sphagnum cores that did not have this abrupt transition with depth (Figures 2 and 5 and Table S4). Sphagnum moss typically has a very low nitrogen concentration and as such has a high C:N ratio (Watmough et al. 2022), which also distinguishes the two control treatment types and is therefore related to CO₂ fluxes. Low C:N ratios are also associated with more decomposed peat, which would have a higher ρ_d , lowering porosity, and lower proportion of macropores (Wang et al. 2015). Elevated CO₂ fluxes in peat exhibiting a high ρ_d are consistent with past mesocosm experiments, where more compressed peat had greater water table fluctuations and deeper oxygen

penetration during drying events over a certain threshold, leading to more respiration (Estop-Aragonés et al. 2016; Scanlon and Moore 2000). Decomposability of peat types may also play a role, where *Sphagnum* moss generally has a lower decomposition rate than other common moss types, especially in hummock species (Turetsky et al. 2008).

The absence of a low ρ_d and high porosity surficial cover (compared to both control treatments) is apparent in the mulched treatments (Figures 4 and 5). This is indicative of disturbance to the peat hydrophysical structure due to the combined impacts of mulching, mixing, peat removal and/or compression which occurs during the creation of the seismic line, as noted in previous studies on linear disturbances (Strack et al. 2018; Davidson et al. 2020). The comparable peat composition (Figure 3) and muted disturbance to hydrophysical properties in the mechanically roughed Sphagnum is likely due to the presence of surficial mechanical mixing only without the added effects of mulching and compression arising from mulchers passing over the surface during seismic line construction. Compression is likely an explanatory factor for the elevated bulk density of the mulched samples (Figure 4a), whereas the incorporation of mulched material likely resulted in the lower C:N (Tables 1 and S5) and increased proportions of UOM and root material (Figures 3, 5 and S2) compared to the controls and RGH-SPH, as the proportions of both increased with degree of mulching (MUL-HI when compared to MUL-LOW). Though CO2 fluxes were not significantly different than the feathermoss-dominated control, the absence of large proportions of feathermoss in the MUL-LOW and MUL-HI cores suggests prior to disturbance these may have exhibited structural similarities to the Sphagnum-dominated

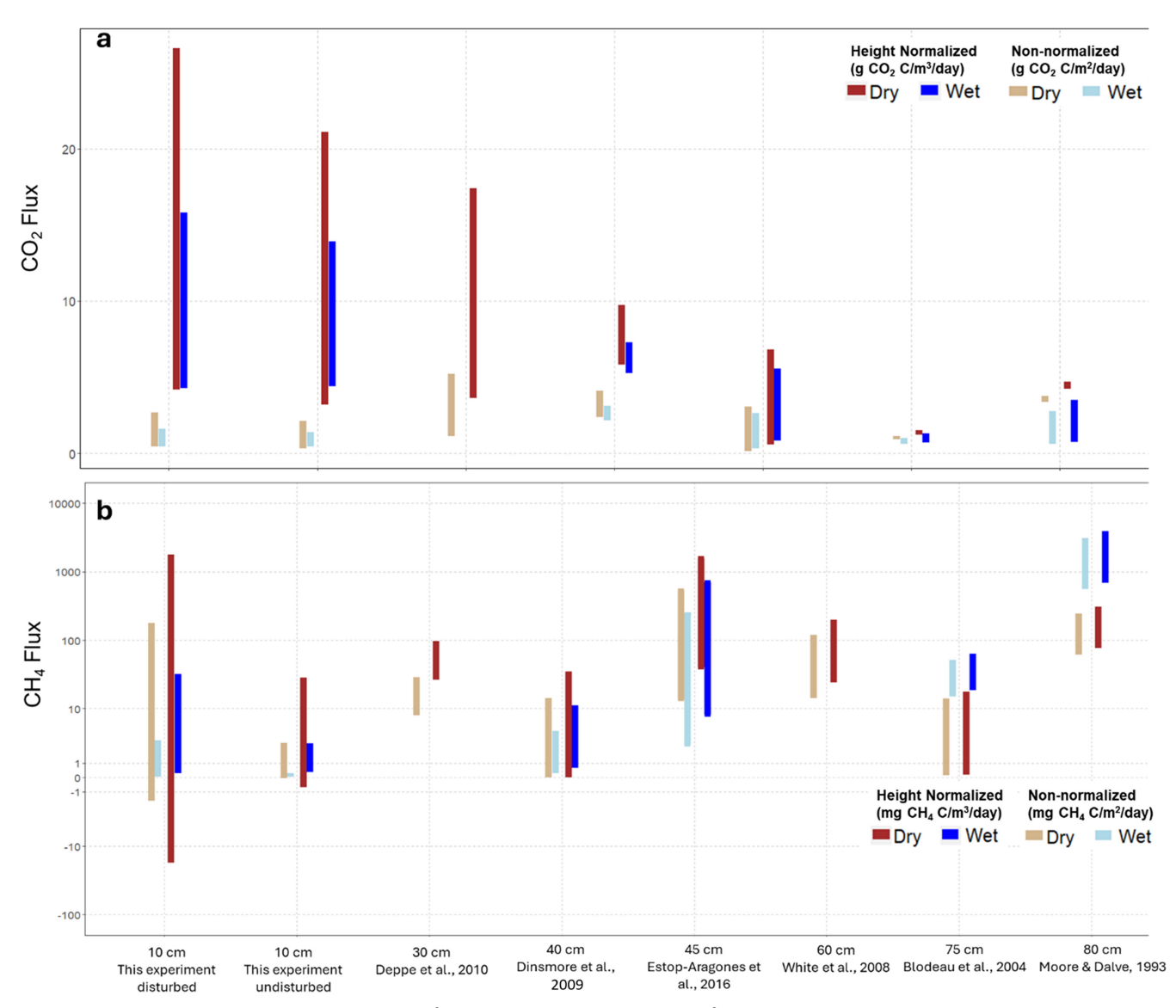


FIGURE 6 | Ranges of height normalized (g·C/m³/day) and non-normalized (g·C/m²/day) (a) CO_2 flux and (b) CH_4 flux from northern hemisphere poor fen and bog peat core experiments across varying core heights and water table conditions (here grouped into wet [<5cm bgs] and dry [>5cm·bgs]). Literature dry conditions ranged from 18 to 40 cm·bgs. Note the logarithmic scale for CH_4 fluxes.

controls, thus highlighting the importance of vegetation community composition as well as disturbance when characterizing disturbance-induced changes to carbon cycling.

4.1.1 | CH₄ Dynamics and the Influence of Hydrophysical Structure and Disturbance

The large range of $\mathrm{CH_4}$ fluxes, both within and among treatments (Figure 2 and Table S3), is consistent with the large range reported in other literature mesocosm experiments (Figure 6b; Moore and Dalva 1993; Blodau et al. 2004; Dinsmore et al. 2009; Deppe et al. 2010; Estop-Aragonés et al. 2016; White et al. 2008). Whereas wet $\mathrm{CH_4}$ fluxes were generally on the low end of literature values, fluxes were larger, more variable and in the disturbed treatments dominated by a small number of large measurements in a subset of cores during the dry condition. This contrasts with the majority of comparable mesocosm studies which reported decreased $\mathrm{CH_4}$ emissions at deeper water tables (Blodau

et al. 2004; Dinsmore et al. 2009; Moore and Dalva 1993; White et al. 2008). However, a smaller number of previous mesocosm experiments also reported increased $\mathrm{CH_4}$ emissions after water table lowering via large episodic events (Hermans et al. 2019; Deppe et al. 2010; Estop-Aragonés et al. 2016) resulting in fluxes spanning > 3 orders of magnitude (Figure 6b). The apparent increase of $\mathrm{CH_4}$ flux in this experiment was likely attributable to the release of trapped $\mathrm{CH_4}$ during measurement that was generated between flux events, consistent with the larger standard deviation in most cores post drying.

The explanation of increased ${\rm CH_4}$ fluxes due to a release of trapped ${\rm CH_4}$ during flux measurement events in the dry condition can be seen best in the relation between fluxes and the hydrophysical and compositional characteristics of the cores. The three cores with large ${\rm CH_4}$ flux events (MUL-HI-2, MUL-LOW-2 and MUL-LOW-4 in Table S4) had high ρ_d , and low measures of porosity/ \mathcal{R}_m (Figure 4a,b,d), indicative of peat with lower overall pore volumes and pore networks dominated by small and/or

closed pores more likely to trap $\mathrm{CH_4}$ gas produced between flux events than looser, high-porosity surface peat. Compositionally, higher than average proportions of roots near the surface of these cores (Figure S2) may have further facilitated the release of $\mathrm{CH_4}$ produced at the bottom of the cores, particularly after desaturating after water table lowering. In turn, the bottom peat in these cores had lower than average C:N ratios (Tables 1 and S5), and both sub-cores had higher than average proportions of herbs, woody material and UOM (Figure S2), decomposable material likely introduced through mulching and/or mixing.

The accumulation of CH₄ underneath dense (and likely lowporosity) peat was observed in Strack and Mierau (2010), in which significantly higher concentrations of porewater CH₄ were detected underneath poor fen ridges when compared to hollows, which they attributed to woody roots and more tightly packed Sphagnum species in the former creating a confining layer. The entrapment and subsequent release of CH4 was observed in Estop-Aragonés et al. (2012), in which porewater CH concentrations increased during the high water table condition and subsequently declined shortly after water table lowering, which coincided with large CH, emissions from the core surface. Increased CH4 emissions were not observed during peat rewetting or with static but deep-water tables (Estop-Aragonés et al. 2012), speaking to the strongly hysteretic nature of this behaviour. As we did not measure CH4 flux during the water table lowering directly, potential release of CH4 was not captured during this study; however, given the observations of ebullitive fluxes later in the experiment, this release likely would have occurred.

Though not directly confirmed here, peat that is more compacted and has a greater proportion of smaller pores (noted in our mulched cores; Figures 4c,d and S3) may also increase the production of CH₄ through the increased presence of methanogenesis-favouring microenvironments in closed pore spaces (Knorr et al. 2008; Estop-Aragonés et al. 2016) that may remain saturated even after dewatering due to a high water retention capacity (Deppe et al. 2010).

4.1.2 | Scalability of Results to Field Studies and Modelling Efforts

Like the results of this experiment, field studies on linear disturbances have reported similar or lower CO_2 emissions online compared to adjacent undisturbed peatlands, even in areas exhibiting increased bulk density and compression (Strack et al. 2018; Korsah 2023). It appears that warmer temperatures and significantly shallower water tables online are overriding factors to the potential for increased CO_2 production due to the denser and more labile peat that may be present at the surface of disturbance.

Though increased $\mathrm{CH_4}$ emissions have been documented on linear disturbances, the link to peat composition and hydrophysical structure is less so. In a winter road investigation (Strack et al. 2018), an increase in $\mathrm{CH_4}$ flux was attributed to warmer temperatures and increased graminoid cover, the latter likely a function of the shallower water tables on the line. Though not directly measured, the wetter conditions on the line were likely

a result of the decreased porosity and increased water retention of the higher density disturbed peat, supported by our experimental findings as well as field characterization on seismic line disturbances (Davidson et al. 2020) that showed similar changes to hydrophysical properties and water table elevation. More direct relationships between water table depth and CH4 flux were measured in Schmidt et al. 2022 and related to line flattening and compression, also likely related to similar changes in hydrophysical structure. The relative absence of ebullitive emissions in previous field studies is interesting and likely due to the short time period and relatively sparse intervals in which plot-scale fluxes are measured in the field. Limited ebullitive events were captured in one field study on seismic line disturbed peatlands (Schmidt et al. 2022); however, the dominance of ebullitive events on average CH, flux in our disturbed treatments suggests the need for further exploration of these processes at a field scale as field emissions may be currently underestimated by orders of magnitude.

As noted in this experiment, significant differences in peat hydrophysical structure, composition and CO2/CH4 fluxes occurred between control treatments of different cover (i.e., Sphagnum vs. feathermoss). Though unlikely to be a factor in the collected cores due to the relative age of the seismic line during sample collection (1-year post-disturbance), these results suggest that over time, long-term vegetation shifts may become an equally important variable in quantifying disturbance as the direct alteration to peat properties. In the field, the opening of the canopy during tree removal has the potential to shift moss cover from feathermoss to Sphagnum (Bisbee et al. 2001), which is generally more recalcitrant (Turetsky et al. 2008) here shown to have lower CO2 and CH4 fluxes (Figures 2 and 3). However, wetter conditions due to compaction and increased water retention (van Rensen et al. 2015; Strack et al. 2018; Schmidt et al. 2022), combined with the introduction of lower C:N peat to the surface in the peat substrate due to mulching and mixing, offset this potential for emissions reduction. Finally, the introduction of more easily decomposed vascular vegetation can provide more substrate for CH₄ production (Strack et al. 2017), further increasing CH₄ emissions.

5 | Limitations and Future Work

The authors acknowledge that both wet and dry water tables are within the upper range of natural conditions in undisturbed poor fens in the Alberta region and therefore may not capture the full range of carbon cycling dynamics possible in these ecosystems. The water table ranges presented here are, however, reflective of on-line conditions reported in-field on linear disturbances (Williams et al. 2013; van Rensen et al. 2015; Lovitt et al. 2018; Strack et al. 2018) and oil sands exploration well sites (Murray et al. 2021). Therefore, the bias towards wetter moisture conditions in this study is a reasonable reflection of expected field conditions.

To properly analyse the influence of peat structure and composition on carbon cycling, water tables were held constant for each moisture condition, and temperature was held at 20°C \pm 3°C for the duration of the experiment. Future research could benefit from a longer temporal scope to capture seasonal variations and long-term trends in $\rm CO_2$ and $\rm CH_4$ fluxes. In field conditions,

both water table and temperature variability have strong influences on carbon cycling dynamics; therefore, field studies that quantify both changes to peat composition and variations in environmental conditions could offer a more comprehensive understanding of these processes.

Under dry conditions, average fluxes in the MUL-LOW and MUL-HI cores were biased by a few disproportionately large episodic events. These events were temporally inconsistent, meaning not all episodic emissions were likely captured during measurement, particularly given the lack of data from the equilibrium phase following water table lowering where previous studies have reported ebullition events (Estop-Aragonés et al. 2012). The strong influence of core structure and composition on the presence of these large emissions suggests that any missed episodic CH, fluxes likely occurred in the same cores where they have already been observed. Although the actual CH₄ flux in these cores therefore may be higher than measured, the emissions captured are still likely representative of comparisons between treatments. Future studies specifically targeting patterns and pathways of CH₄ fluxes would provide valuable insights into the actual magnitude and dynamics of these emissions.

Last, the authors acknowledge the uncertainties present in attempting to capture $\mathrm{CH_4}$ fluxes across a gradient of disturbance at a core scale given the heterogeneous nature of the landscape and $\mathrm{CH_4}$ production in general. As such, there is an inherent risk in the scaling up of these data to a regional scale; this information should therefore be used to infer general patterns and increase the accuracy of current estimates; however, values should not be assumed to adequately represent all larger scale processes inherent in these systems.

6 | Conclusions

Within the bounds of this experiment, variations in peat composition and hydrophysical structure were strong predictors of GHG emissions (i.e., CO_2 and CH_4) in cores from the upper 10 cm of natural and seismic line disturbed fen peat, overriding the influence of water availability measured as water table depth. Elevated CO_2 emissions were associated with peat that exhibited a high bulk density, low total and effective porosity and relatively low C:N ratio. In the undisturbed treatments, peat of this structure was observed in the bottom portion of feathermoss-dominated cores associated with a vegetational shift with increasing depth. In the disturbed treatments, the peat of this structure was observed in the surface as well as at depth and is likely attributable to the processes of mulching, mixing and compression as part of seismic line creation.

The relationship between peat type/hydrophysical structure and $\mathrm{CH_4}$ emissions was more complex as emissions were dominated by a small number of episodic events that only occurred in mulched cores during the low water table conditions. It is likely that the disruption in pore structure near the surface of these cores (observed through reduced effective porosity and percentage of macropores) trapped gas containing $\mathrm{CH_4}$ within closed pores. After water tables were lowered, pore desaturation allowed for the release of this trapped $\mathrm{CH_4}$ during flux measurement events.

The findings of this research suggest using caution when mulching on seismic lines and incorporating mulch within the near surface. At the lab scale, the incorporation of mulch decreased C:N ratios and increased UOM and root material. This drove elevated CO2 fluxes and, when combined with compaction, also increased CH₄ entrapment and ebullition events. At a field scale, the direct impact of altered hydrophysical structure on CO₂ and CH₄ emissions is likely to be muted due to the combined effects of additional environmental change, such as increasing online temperatures, and changes to plant community structure. Additional work should therefore be conducted on a field scale to further assess the interrelationships between direct changes to hydrophysical structure and these other impacts to better determine the long-term alterations to carbon cycling in systems disturbed by seismic line creation. Further, the time in which it takes for the growth of new vegetation to re-establish a near-surface peat hydrophysical structure more similar to undisturbed peatlands should be assessed in order to gain a better understanding of the duration of impact for this type of disturbance.

Acknowledgements

The authors would like to acknowledge funding from Environment and Climate Change Canada. We would like to thank Lyna Lapointe-Elmrabti and Kelly Bona for their assistance with experiment development and providing their feedback on this manuscript. We would like to thank Marayam Bayatvarkeshi and Nazia Tabassum for their efforts in sample collection and the many laboratory assistants who lent their support during experiment execution. Samples for this study were collected from the unceded territories of the peoples of the Treaty 8 region and Métis Nation of Alberta, and the laboratory portion of this work took place on the unceded traditional territory of the Attawandaron (Neutral), Anishinaabeg and Haudenosaunee peoples.

Data Availability Statement

The data that supports the findings of this study are available in the supplementary material of this article.

References

Alberta Biodiversity Monitoring Institute. 2021. "ABMI Alberta Wetland Inventory Data." Last modified March 31. https://abmi.ca/data-portal/40.html.

Bear, J. 1972. "Dynamics of Fluids in Porous Materials." Society of Petroleum Engineers.

Bieniada, A., and M. Strack. 2021. "Steady and Ebullitive Methane Fluxes From Active, Restored and Unrestored Horticultural Peatlands." *Ecological Engineering* 169: 106324.

Bisbee, K. E., S. T. Gower, J. M. Norman, and E. V. Nordheim. 2001. "Environmental Controls on Ground Cover Species Composition and Productivity in a Boreal Black Spruce Forest." *Oecologia* 129: 261–270. https://doi.org/10.1007/s004420100719.

Blodau, C., N. Basiliko, and T. R. Moore. 2004. "Carbon Turnover in Peatland Mesocosms Exposed to Different Water Table Levels." *Biogeochemistry* 67: 331–351.

Boelter, D. H. 1969. "Physical Properties of Peats as Related to Degree of Decomposition." *Soil Science Society of America Journal* 33: 606–609. https://doi.org/10.2136/sssaj1969.03615995003300040033x.

Bridgham, S. D., H. Cadillo-Quiroz, J. K. Keller, and Q. Zhuang. 2013. "Methane Emissions From Wetlands: Biogeochemical, Microbial, and

Modeling Perspectives From Local to Global Scales." *Global Change Biology* 19: 1325–1346.

Bubier, J. L., T. R. Moore, and N. T. Roulet. 1993. "Methane Emissions From Wetlands in the Midboreal Region of Northern Ontario, Canada." *Ecology* 74, no. 8: 2240–2254.

Caners, R. T., and V. J. Lieffers. 2014. "Divergent Pathways of Successional Recovery for In Situ Oil Sands Exploration Drilling Pads on Wooded Moderate-Rich Fens in Alberta, Canada." *Restoration Ecology* 22, no. 5: 657–667.

Clymo, R. S. 1983. "Peat." In *Ecosystems of the World*, 4A. Mires: Swamp, Bog, Fen and Moor, General Studies, edited by A. J. P. Gore, 159–224. Elsevier.

Clymo, R. S. 1996. "Assessing the Accumulation of Carbon in Peatlands." In Northern Peatlands in Global Climate Change, edited by R. Laiho, J. Laine, and H. Vasander, 207–212. SILMU.

Clymo, R. S., and D. M. E. Pearce. 1995. "Methane and Carbon Dioxide Production in, Transport Through, and Efflux From a Peatland." *Philosophical Transactions of the Royal Society of London. Series a: Physical and Engineering Sciences* 351, no. 1696: 249–259.

Dabros, A., M. Pyper, and G. Castilla. 2018. "Seismic Lines in the Boreal and Arctic Ecosystems of North America: Environmental Impacts, Challenges, and Opportunities." *Environmental Reviews* 26: 214–229. https://doi.org/10.1139/er-2017-0080.

Davidson, S. J., E. M. Goud, C. Franklin, S. E. Nielsen, and M. Strack. 2020. "Seismic Line Disturbance Alters Soil Physical and Chemical Properties Across Boreal Forest and Peatland Soils." *Frontiers in Earth Science* 8: 281.

Deppe, M., K. H. Knorr, D. M. McKnight, and C. Blodau. 2010. "Effects of Short-Term Drying and Irrigation on CO_2 and CH_4 Production and Emission From Mesocosms of a Northern Bog and an Alpine Fen." *Biogeochemistry* 100: 89–103.

Dinsmore, K. J., U. M. Skiba, M. F. Billett, and R. M. Rees. 2009. "Effect of Water Table on Greenhouse Gas Emissions From Peatland Mesocosms." *Plant and Soil* 318: 229–242.

Estop-Aragonés, C., K. H. Knorr, and C. Blodau. 2012. "Controls on In Situ Oxygen and Dissolved Inorganic Carbon Dynamics in Peats of a Temperate Fen." *Journal of Geophysical Research: Biogeosciences* 117, no. 2: 1–14. https://doi.org/10.1029/2011JG001888.

Estop-Aragonés, C., K. Zając, and C. Blodau. 2016. "Effects of Extreme Experimental Drought and Rewetting on ${\rm CO_2}$ and ${\rm CH_4}$ Exchange in Mesocosms of 14 European Peatlands With Different Nitrogen and Sulfur Deposition." *Global Change Biology* 22, no. 6: 2285–2300.

Frolking, S., and N. T. Roulet. 2007. "Holocene Radiative Forcing Impact of Northern Peatland Carbon Accumulation and Methane Emissions." *Global Change Biology* 13, no. 5: 1079–1088.

Gharedaghloo, B., and J. S. Price. 2019. "Characterizing the Immiscible Transport Properties of Diesel and Water in Peat Soil." *Journal of Contaminant Hydrology* 221: 11–25.

Goetz, J. D., and J. S. Price. 2015. "Role of Morphological Structure and Layering of *Sphagnum* and *Tomenthypnum* Mosses on Moss Productivity and Evaporation Rates." *Canadian Journal of Soil Science* 95, no. 2: 109–124.

Hayward, P. M., and R. S. Clymo. 1982. "Profiles of Water Content and Pore Size in *Sphagnum* and Peat, and Their Relation to Peat Bog Ecology." *Proceedings of the Royal Society of London, Series B: Biological Sciences* 215, no. 1200: 299–325.

Hermans, R., N. Zahn, R. Andersen, Y. A. Teh, N. Cowie, and J. A. Subke. 2019. "An Incubation Study of GHG Flux Responses to a Changing Water Table Linked to Biochemical Parameters Across a Peatland Restoration Chrono Sequence." *Mires and Peat* 23: 8–18.

Hogg, E. H. 1993. "Decay Potential of Hummock and Hollow *Sphagnum* Peats at Different Depths in a Swedish Raised Bog." *Oikos* 66: 269–278.

Hogg, E. H., V. J. Lieffers, and R. W. Wein. 1992. "Potential Carbon Losses From Peat Profiles: Effects of Temperature, Drought Cycles, and Fire." *Ecological Applications* 2: 298–306.

Holden, J. 2009. "Flow Through Macropores of Different Size Classes in Blanket Peat." *Journal of Hydrology* 364, no. 3–4: 342–348.

Howard, D. M., and P. J. A. Howard. 1993. "Relationships Between CO₂ Evolution, Moisture Content and Temperature for a Range of Soil Types." *Soil Biology and Biochemistry* 25: 1537.

Hugelius, G., J. Loisel, S. Chadburn, et al. 2020. "Large Stocks of Peatland Carbon and Nitrogen Are Vulnerable to Permafrost Thaw." *Proceedings of the National Academy of Sciences* 117, no. 34: 20438–20446.

Ingram, H. A. P. 1978. "Soil Layers in Mires: Function and Terminology." *European Journal of Soil Science* 29: 224–227. https://doi.org/10.1111/j. 1365-2389.1978.tb02053.x.

IPCC. 2014. In 2013 Supplement to the 2006 IPCC Guidelines for National Greenhouse Gas Inventories, edited by T. Wetlands-Hiraishi, T. Krug, K. Tanabe, N. Srivastava, J. Baasansuren, M. Fukuda, and T. G. Troxler. IPCC.

Kettunen, A., V. Kaitala, A. Lehtinen, et al. 1999. "Methane Production and Oxidation Potentials in Relation to Water Table Fluctuations in Two Boreal Mires." *Soil Biology and Biochemistry* 31, no. 12: 1741–1749.

Knorr, K. H., M. R. Oosterwoud, and C. Blodau. 2008. "Experimental Drought Alters Rates of Soil Respiration and Methanogenesis but Not Carbon Exchange in Soil of a Temperate Fen." *Soil Biology and Biochemistry* 40, no. 7: 1781–1791.

Korsah, P 2023. "Effects of Seismic Lines on Peatland Carbon Cycling in Boreal Alberta, Canada." Doctoral thesis.

Larmola, T., J. L. Bubier, C. Kobyljanec, et al. 2013. "Vegetation Feedbacks of Nutrient Addition Lead to a Weaker Carbon Sink in an Ombrotrophic Bog." *Global Change Biology* 19, no. 12: 3729–3739.

Lee, P., and S. Boutin. 2006. "Persistence and Developmental Transition of Wide Seismic Lines in the Western Boreal Plains of Canada." *Journal of Environmental Management* 78: 240–250. https://doi.org/10.1016/j.jenvman.2005.03.016.

Legendre, P., and L. Legendre. 2012. Numerical Ecology. Vol. 24. Elsevier.

Lepilin, D., A. Laurén, J. Uusitalo, and E. S. Tuittila. 2019. "Soil Deformation and Its Recovery in Logging Trails of Drained Boreal Peatlands." *Canadian Journal of Forest Research* 49, no. 7: 743–751.

Lévesque, P. E. M., H. Dinel, and A Larouche. 1988. "Guide to the Identification of Plant Macrofossils in Canadian Peatlands." Ministry of Supply and Services Canada Publication No. 1817, Ottawa, ON, Canada.

Loisel, J., and A. Gallego-Sala. 2022. "Ecological Resilience of Restored Peatlands to Climate Change." *Communications Earth & Environment* 3, no. 1: 208.

Lovitt, J., M. M. Rahman, S. Saraswati, G. J. McDermid, M. Strack, and B. Xu. 2018. "UAV Remote Sensing can Reveal the Effects of Low-Impact Seismic Lines on Surface Morphology, Hydrology and Methane (CH $_4$) Release in a Boreal Treed bog." *Journal of Geophysical Research – Biogeosciences* 123: 1117–1129. https://doi.org/10.1002/2017JG004232.

Mauquoy, D., P. D. M. Hughes, and B. Van Geel. 2010. "A Protocol for Plant Macrofossil Analysis of Peat Deposits." *Mires and Peat* 7, no. 6: 1–5.

McCarter, C. P., and J. S. Price. 2017. "Experimental Hydrological Forcing to Illustrate Water Flow Processes of a Subarctic Ladder Fen Peatland." *Hydrological Processes* 31, no. 8: 1578–1589.

Moore, T. R., and M. Dalva. 1993. "The Influence of Temperature and Water Table Position on Carbon Dioxide and Methane Emissions From Laboratory Columns of Peatland Soils." *European Journal of Soil Science* 44: 651–664.

Murray, K. R., M. Bird, M. Strack, M. Cody, and B. Xu. 2021. "Restoration Approach Influences Carbon Exchange at In-Situ oil Sands Exploration Sites in East-Central Alberta." *Wetlands Ecology and Management* 29: 281–299.

Nungesser, M. K. 2003. "Modelling Microtopography in Boreal Peatlands: Hummocks and Hollows." *Ecological Modelling* 165, no. 2–3: 175–207.

Oksanen, P., F. G. Blanchet, M. Friendly, et al. 2018. "vegan: Community Ecology Package." R Package Version 2.5-2.

Price, J. S., P. N. Whittington, D. E. Elrick, M. Strack, N. Brunet, and E. Faux. 2008. "A Method to Determine Unsaturated Hydraulic Conductivity in Living and Undecomposed *Sphagnum Moss.*" *Soil Science Society of America Journal* 72, no. 2: 487–491.

Quinton, W. L., T. Elliot, J. S. Price, F. Rezanezhad, and R. Heck. 2009. "Measuring Physical and Hydraulic Properties of Peat From X-Ray Tomography." *Geoderma* 153, no. 1–2: 269–277.

R Core Team. 2021. "R: A Language and Environment for Statistical Computing." R Foundation for Statistical Computing, Vienna, Austria. https://www.R-project.org/.

Rezanezhad, F., J. S. Price, W. L. Quinton, B. Lennartz, T. Milojevic, and P. Van Cappellen. 2016. "Structure of Peat Soils and Implications for Water Storage, Flow and Solute Transport: A Review Update for Geochemists." *Chemical Geology* 429: 75–84.

Rezanezhad, F., W. L. Quinton, J. S. Price, T. R. Elliot, D. Elrick, and K. R. Shook. 2010. "Influence of Pore Size and Geometry on Peat Unsaturated Hydraulic Conductivity Computed From 3D Computed Tomography Image Analysis." *Hydrological Processes* 24, no. 21: 2983–2994.

Scanlon, D., and T. Moore. 2000. "Carbon Dioxide Production From Peatland Soil Profiles: The Influence of Temperature, Oxic/Anoxic Conditions and Substrate." *Soil Science* 165, no. 2: 153–160.

Schmidt, M., S. J. Davidson, and M. Strack. 2022. " $\rm CO_2$ Uptake Decreased and $\rm CH_4$ Emissions Increased in First Two Years of Peatland Seismic Line Restoration." Wetlands Ecology and Management 30, no. 2: 313–329.

Severson-Baker, C. 2003. "Seismic Exploration Environment & Energy in the North." The Pembina Institute Box 7558, Drayton Valley, AB T7A 1S7.

Strack, M., S. Hayne, S. Lovitt, et al. 2019. "Petroleum Exploration Increases Methane Emissions From Northern Peatlands." *Nature Communications* 10: 2804. https://doi.org/10.1038/s41467-019-10762-4.

Strack, M., and T. Mierau. 2010. "Evaluating Spatial Variability of Free-Phase Gas in Peat Using Ground-Penetrating Radar and Direct Measurement." *Journal of Geophysical Research: Biogeosciences* 115, no. G2: 1–11. https://doi.org/10.1029/2009JG001045.

Strack, M., K. Mwakanyamale, G. Hassanpour Fard, M. Bird, V. Bérubé, and L. Rochefort. 2017. "Effect of Plant Functional Type on Methane Dynamics in a Restored Minerotrophic Peatland." *Plant and Soil* 410: 231–246.

Strack, M., D. Softa, M. Bird, and B. Xu. 2018. "Impact of Winter Roads on Boreal Peatland Carbon Exchange." *Global Change Biology* 24, no. 1: e201–e212.

Sundh, I., M. Nilsson, G. Granberg, and B. H. Svensson. 1994. "Depth Distribution of Microbial Production and Oxidation of Methane in Northern Boreal Peatlands." *Microbial Ecology* 27: 253–265.

Turetsky, M. R., S. E. Crow, R. J. Evans, D. H. Vitt, and R. K. Wieder. 2008. "Trade-Offs in Resource Allocation Among Moss Species Control Decomposition in Boreal Peatlands." *Journal of Ecology* 96: 1297–1305. https://doi.org/10.1111/j.1365-2745.2008.01438.x.

Updegraff, K., J. Pastor, S. D. Bridgham, and C. A. Johnston. 1995. "Environmental and Substrate Controls Over Carbon and Nitrogen Mineralization in Northern Wetlands." *Ecological Applications* 5: 151–163.

van Rensen, C. K., S. E. Nielsen, B. White, T. Vinge, and V. J. Lieffers. 2015. "Natural Regeneration of Forest Vegetation on Legacy Seismic Lines in Boreal Habitats in Alberta's Oil Sands Region." *Biological Conservation* 184: 127–135. https://doi.org/10.1016/j.biocon.2015. 01.020.

Waddington, J. M., N. T. Roulet, and R. V. Swanson. 1996. "Water Table Control of CH₄ Emission Enhancement by Vascular Plants in Boreal Peatlands." *Journal of Geophysical Research-Atmospheres* 101: 22775–22785.

Wang, M., T. R. Moore, J. Talbot, and J. Riley. 2015. "The Stoichiometry of Carbon and Nutrients in Peat Formation." *Global Biogeochemical Cycles* 29, no. 2: 113–121. https://doi.org/10.1002/2014GB005000.

Watmough, S., S. Gilbert-Parks, N. Basiliko, L. J. Lamit, et al. 2022. "Variation in Carbon and Nitrogen Concentrations Among Peatland Categories at a Global Scale." *PLoS ONE* 17, no. 11: e0275149.

Weedon, J. T., R. Aerts, G. A. Kowalchuk, R. van Logtestijn, D. Andringa, and P. M. van Bodegom. 2013. "Temperature Sensitivity of Peatland C and N Cycling: Does Substrate Supply Play a Role?" *Soil Biology and Biochemistry* 61: 109–120.

White, J. R., R. D. Shannon, J. F. Weltzin, J. Pastor, and S. D. Bridgham. 2008. "Effects of Soil Warming and Drying on Methane Cycling in a Northern Peatland Mesocosm Study." *Journal of Geophysical Research* 113: 1–18. https://doi.org/10.1029/2007JG000609.

Whittington, P., A. Koiter, D. Watts, A. Brewer, and V. Golubev. 2021. "Bulk Density, Particle Density, and Porosity of Two Species of *Sphagnum*: Variability in Measurement Techniques and Spatial Distribution." *Soil Science Society of America Journal* 85, no. 6: 2220–2233.

Wilkinson, S. L., C. P. R. McCarter, M. Taufik, A. Noble, F. Nwaishi, and S. J. Davidson. 2023. "Climate Impacts of Anthropogenic Disturbances: Understudied Anthropogenic Disturbances and Peatland Carbon Cycling." In *Peatlands and Climate Change*, edited by M. Strack, 2nd ed., 112–151. International Peatland Society.

Williams, T. J., W. L. Quinton, and J. L. Baltzer. 2013. "Linear Disturbances on Discontinuous Permafrost: Implications for Thaw-Induced Changes to Land Cover and Drainage Patterns." *Environmental Research Letters* 8: 025006. https://doi.org/10.1088/1748-9326/8/2/025006.

Supporting Information

Additional supporting information can be found online in the Supporting Information section.